Comparison between effective doses for voxel-based and stylized exposure models from photon and electron irradiation

R Kramer [1], H J Khoury [1] and J W Vieira [2,3]

[1] Departamento de Energia Nuclear, Universidade Federal de Pernambuco, Av. Prof. Luiz Freire 1000, Cidade Universitária, CEP: 50740-540, Recife, PE, Brazil

[2] Centro Federal de Educação Tecnológica de Pernambuco, Recife, PE, Brazil

[3] Escola Politécnica, UPE, Recife, PE, Brazil

E-mail: rkramer@uol.com.br

Statement of provenance:
'This is an author-created, un-copyedited version of an article accepted for publication in Physics in Medicine and Biology. IOP Publishing Ltd is not responsible for any errors or omissions in this version of the manuscript or any version derived from it. The definitive publisher authenticated version is available at doi:10.1088/0031-9155/50/21/011. '

ABSTRACT

For the last two decades organ and tissue equivalent dose as well as effective dose conversion coefficients recommended by the International Commission on Radiological Protection (ICRP) have been determined with exposure models based on stylized MIRD5-type phantoms representing the human body with its radiosensitive organs and tissues according to the ICRP Reference Man released in Publication 23, on Monte Carlo codes sometimes simulating rather simplified radiation physics, and on tissue compositions from different sources. Meanwhile the International Commission on Radiation Units and Measurements (ICRU) has published reference data for human tissue compositions in Publication No.44, and the ICRP has released a new report on anatomical reference data in Publication 89. As a consequence many of the components of the traditional stylized exposure models used to determine the effective dose in the past have to be replaced: Monte Carlo codes, human phantoms and tissue compositions. This paper presents results of comprehensive investigations on the dosimetric consequences to be expected from the replacement of traditional stylized exposure models by voxel-based exposure models. Calculations have been performed with the EGS4 Monte Carlo codes for external and internal exposures to photons and electrons with the stylized, gender-specific MIRD5-type phantoms ADAM and EVA on the one hand, and with the recently developed tomographic or voxel-based phantoms MAX and FAX on the other hand for a variety of exposure conditions. Ratios between effective doses for the voxel-based and the stylized exposure models will be presented for external and internal exposures to photons and electrons as function of the energy and the geometry of the radiation field. The data indicate that for the exposure conditions considered in these investigations the effective dose may change between +60% and –50% after the replacement of the traditional exposure models by the voxel-based exposure models.

1. Introduction

Conversion coefficients (CCs) between effective dose and physical quantities characterizing the radiation source or field have been published by the International Commission on Radiological Protection (ICRP) for external and internal exposures in order to facilitate the interpretation of data measured in routine radiation protection in terms of the primary protection quantity (ICRP 1995a, 1996a, 1996b).

This primary protection quantity, the effective dose, "is the sum of the weighted equivalent doses in all tissues and organs of the body. It is given by the expression

$$E = \sum_T w_T H_T$$

where H_T is the equivalent dose in tissue or organ T and w_T is the weighting factor for tissue T" (ICRP 1991).

According to Table 1, the ICRP recommends tissue weighting factors for 13 selected tissues and organs, plus one single tissue weighting factor for a so-called "remainder", which is composed of another 10 organs and tissues. The quantity H_T represents the equivalent dose averaged over the volume of tissue T, which reflects the assumption of a linear dose-risk relationship.

Table 1. Tissue weighting factors from ICRP60

Tissue/Organ	w_T
Gonads	0.20
RBM, Colon, Lungs, Stomach	0.12
Bladder, Breast, Liver, Oesopagus, Thyroid	0.05
Skin, Bone surface	0.01
Remainder	0.05

Remainder: adrenals, brain, trachea, small intestine, muscle, pancreas, kidneys, spleen, thymus, uterus

Effective dose CCs have been calculated by applying Monte Carlo radiation transport methods to virtual representations of the human body, so-called mathematical or stylized phantoms. In stylized human phantoms size and form of the body and its organs are described by mathematical expressions representing combinations and intersections of planes, circular and elliptical cylinders, spheres, cones, tori, etc.

Fisher and Snyder (1967,1968) introduced this type of phantom for an adult male which also contained ovaries and a uterus. During the compilation of the Report of the Task Group on Reference Man, Publication No.23 (ICRP 1975) the phantom has been further developed by Snyder et al (1974,1978). Since then it is known as "MIRD5 phantom" (*M*edical *I*nternal *R*adiation *D*ose Committee (MIRD) Pamphlet No. 5). The MIRD5 phantom has been the basis for various derivations representing infants and children of various ages (Cristy 1980), gender-specific adult phantoms, called ADAM and EVA (Kramer et al 1982), and a pregnant female adult phantom (Stabin et al 1995). Body height and weight as well as the organ masses of MIRD5-type phantoms are in accordance with the Reference Man data from Publication 23 (ICRP 1975).

Mainly the gender-specific ADAM and EVA phantoms have been used for the calculations of the CCs for external exposures to photons and electrons recommended by the ICRP in its Publication 74 (ICRP 1996a). The ADAM phantom was derived from the hermaphrodite MIRD5 phantom (Snyder et al 1978) but with female organs (ovaries and uterus) removed, while the EVA phantom is a scaled-down version of the ADAM phantom, to which

ovaries, breasts and a uterus have been added after the removal of the testes. The original MIRD5 phantom had no female breasts.

CCs for internal exposures to photons and electrons have been calculated with a 15 year old hermaphrodite MIRD5 phantom (Cristy and Eckerman 1987), and have been published in ICRP reports (1995a, 1996b) or MIRD5 pamphlets (Snyder et al 1975).

This paper presents ratios between effective doses calculated for the MAX and FAX phantoms on the one hand, and for the ADAM and EVA phantoms on the other hand, in order to show the dosimetric consequences when stylized exposure models will be replaced by voxel-based models. Actually this replacement consists of substituting the Monte Carlo code, the elemental composition of body tissues, the human anatomy, and the distribution of skeletal tissues as well as of adipose and muscle. Investigations of the dosimetric consequences for the effective dose from these four substitutions separately have already been shown elsewhere (Kramer et al 2005a,b,c, Lima et al 2005). The data presented here will summarize these results, but in addition this study presents new results, which are the tables with the organ equivalent dose ratios, and an extensive discussion of the dosimetric implications for all organs and tissues of the main group from table 1.

2. Materials and methods

2.1 The MAX and the FAX phantoms

The MAX phantom has been developed (Kramer et al 2003) based on segmented images from a male patient (Zubal et al 1994), while the FAX phantom has been segmented based on CT images of a female patient (Kramer et al 2004a). After segmentation the volumes of the radiosensitive organs and tissues have been adjusted in order to match the reference masses defined by ICRP89 (ICRP 2003). The phantoms have heterogeneously structured skeletons with voxel-specific skeletal tissue compositions based on masses, percentage distributions, and cellularity factors from ICRP70 (ICRP 1995b). This was achieved by use of the so-called CT number method (Zankl and Wittmann 2001) as adopted by Kramer et al (2003), which takes advantage of the CT numbers (= grey values) contained in the bone pixels of the CT images. Thereby it was possible to improve the calculation of the equivalent dose to the red bone marrow (RBM). The average equivalent dose to the skeleton is taken as an estimate for the equivalent dose to the bone surface. Dosimetric separation instead of geometric segmentation allows for the calculation of skin equivalent dose in the 1.5 mm surface layer of the MAX phantom, and in the 1.2mm surface layer of the FAX phantom, although both phantoms consist of cubic voxels with a thickness of 3.6mm. When an energy deposition has been registered in one of the surface voxels, a special algorithm verifies if the interaction of the particle took place within a depth of 1.5mm or 1.2mm, respectively. If so, then the energy is deposited in skin tissue, otherwise in adipose or breast tissue. This method calculates the equivalent dose to the 1.5mm or 1.2mm skin layer exactly, but a small error occurs with regard to the energy which is deposited in adipose or breast tissue, because the deeper layer of the surface voxel is made of skin tissue. For adipose the additional volume coming from this deeper skin layer represents about 13% of the total adipose volume, for the female breasts about 7%. The densities of skin (1.09 gcm^{-3}) and breast (1.05 gcm^{-3}) are almost the same, i.e. that the error is neglectable. For adipose with a density of 0.95 gcm^{-3} the error of not depositing the correct amount of energy could be somewhat greater, but the equivalent dose to adipose does not contribute to the effective dose. Validation of this method of calculating the equivalent dose to the skin was reported in Kramer et al (2005b). Detailed descriptions of both voxel phantoms are given in Kramer et al (2003, 2004a, 2004b).

2.2 The ADAM and EVA phantoms

The gender-specific adult MIRD5-type phantoms ADAM and EVA have been taken from Kramer et al (1982). Their organ and tissue masses correspond to the anatomical specifications given by the ICRP in its first Reference Man Report, Publication No. 23 (ICRP 1975). The skin thickness is 2mm for both phantoms. The skeleton is homogeneous, and the RBM mass fractions are based on ICRP23. The average equivalent dose to the skeleton is taken as an estimate for the equivalent dose to the bone surface.

2.3 The EGS4 Monte Carlo code

The EGS4 Monte Carlo code (Nelson et al 1985) simulates coupled electron-photon transport through arbitrary media. The default version of EGS4 applies an analogous Monte Carlo method, which was used for the calculations of this investigation. For incident photon radiation Rayleigh scattering has been taken into account and secondary electrons have sometimes been transported using the PRESTA algorithm with ESTEPE = 0.04. The calculations have been performed with 10 million particle per incident energy on a PC with an INTEL Pentium 4, 2 GHz processor. The machine had 500 MB of RAM, although executing the code reqired only about 30 MB. For external exposure simulations the execution times per incident energy were between 10 and 60 minutes for photon energies between 10 keV and 10 MeV using an electron cut-off energy of 200 keV, while for incident electron energies between 100 keV and 1 MeV using an electron cut-off energy of 8 keV, and between 1.5 and 4 MeV using an electron cut-off energy of 200 keV the run times varied between 20 and 80 minutes. The electron cut-off energy of 200 keV for incident photons is necessary for the proper determination of the RBM equivalent dose with the CT number method, without compromising correct equivalent dose calculations to other organs and tissue, which was explained in Kramer et al (2003)

For internal exposures simulations the run times were between 1 and 20 minutes for photons between 10 keV and 4 MeV using KERMA approximation, while for incorporated electrons the execution times were 15 to 35 minutes for energies between 100 keV and 4 MeV, again using elecron cut-off energies of 8 and 200 keV as mentioned above. Photon cut-off energies were 2 keV for incident photons, and 8 keV for incident electrons.

2.4 Elemental composition of body tissues

In Report No. 44 (ICRU 1989) the International Commission on Radiation Units and Measurements (ICRU) has published data on elemental compositions and densities of body tissues, which have been used for the organs and tissues of the MAX and FAX phantoms.

2.5 Exposure models

For any given irradiation the effective dose is primarily a function of the Monte Carlo method applied, of the elemental composition of the body tissues, and of the phantom's anatomy. In order to investigate the dosimetric effects from these three components separately, the following exposure models have been applied to internal and external irradiation with photons and electrons, respectively:

a) The EGS4 Monte Carlo code connected to the ADAM and EVA phantoms with MIRD5-based tissue compositions (Kramer et al 1982).
b) The EGS4 Monte Carlo code connected to the ADAM and EVA phantoms with ICRU44-based tissue compositions.
c) The EGS4 Monte Carlo code connected to the MAX and FAX phantoms with ICRU44-based tissue compositions, with ICRP70-based skeletal tissue distribution, and with separately segmented regions for adipose and muscle.

The results of this investigation (Kramer et al 2005a,b,c, Lima et al 2005) have shown that changes of the effective dose due to different Monte Carlo codes or different tissue compositions are usually smaller than 8% for the most important exposure conditions. The data rather indicate that differences between the anatomies of stylized and voxel-based phantoms are mostly responsible for the major changes to be observed for the effective dose. Therefore the ratios between effective doses for voxel-based and stylized exposure models to be presented in this paper will be analyzed and discussed only in terms of the anatomical differences between the MAX-FAX and the ADAM-EVA phantoms.

2.6 Calculation of effective dose

ICRP Publication 74 (ICRP 1996) recommends to calculate the effective dose based on a relationship suggested by Kramer and Drexler (1982) shown here by equation (1), with the notations B for Breasts, F for Female, M for Male and T for Tissue.

$$E = w_B H_B^F + \sum_{T \neq B} w_T \left(\frac{H_T^M + H_T^F}{2} \right) \qquad (1)$$

$$= w_B H_B^F + \sum_{T \neq B} \frac{w_T H_T^M}{2} + \sum_{T \neq B} \frac{w_T H_T^F}{2}$$

$$= w_B H_B^F + \frac{1}{2} E_M + \sum_{T \neq B} \frac{w_T H_T^F}{2}$$

$$= \frac{1}{2} E_M + \frac{1}{2} w_B H_B^F + \frac{1}{2} w_B H_B^F + \frac{1}{2} \sum_{T \neq B} w_T H_T^F$$

$$= \frac{1}{2} E_M + \frac{1}{2} w_B H_B^F + \frac{1}{2} E_F$$

$$E = \frac{1}{2} \left(E_M + E_F + w_B H_B^F \right) \qquad (2)$$

Calculations of absorbed dose distributions in the human body are usually performed separately for a male and a female phantom. Therefore it is more convenient to use equation (2) for the calculation of the effective dose, which can be derived from equation (1) as shown above.
E_M and E_F are not definitions of "new gender-specific effective doses" to be used in radiological protection. These are mathematical quantities which facilitate the calculation of the effective dose, and consequently for this purpose the tissue weighting factors must not be re-normalized.

2.7 Statistical error

Coefficients of variance (CV) were calculated for all organ and tissue equivalent doses. Their values varied as a function of the size of the organ or tissue, the type of particle, the energy and the direction of incidence. From the main list of table 1 for two groups of organs and tissues,

- large organs (LO): RBM, colon, lungs, liver, stomach, female breasts and skin, and
- small organs (SO): testes, ovaries, bladder and thyroid,

the following CVs have been calculated:

Photons external: For LO the CVs were ca. 1%, except for the female breasts PA: ca. 1-8%.
For SO the CVs were ca. 3-6 %.

Photons internal: The CV depends very much on the source organ. Variations between 1 and 20% were found.

Electrons external: For LO the CVs were ca. 2-3%, except for the femal breastsPA: ca. 3-12%.
For SO the CVs were ca. 5-20%.

Electrons internal: The CV depends very much on the source organ. Variations between 5 and 30% were found.

For the effective dose the CVs were usually 1% for photons, and 1-3% for electrons.

3. Results

3.1 External exposures

CCs between effective dose and air kerma free-in-air or unit particle fluence for external exposures have been calculated with broad parallel beams of photons and electrons uniformly covering the whole body for anterior-posterior (AP) and for posterior-anterior (PA) incidence, as well as for a broad parallel beam rotating 360° around the phantom's vertical axis (ROT). The remainder equivalent dose was calculated as the arithmetic average of the equivalent doses to all the remainder organs and tissues. For very small equivalent doses, if the coefficient of variance (CV) of the equivalent dose of an organ or tissue mentioned in table 1 was greater than 30%, then its equivalent dose was disregarded for the calculations. For given external exposure conditions the equivalent dose to an organ or tissue of the human body is first of all a function of its depth. This is why anatomical differences between phantoms with regard to size, form and location of organs strongly influence dosimetric results. For low incident energies of the radiation only superficial organ and tissues show significant equivalent doses, but with increasing penetration of photons or electrons energy is deposited in deeper lying organs and tissues. For a given energy the penetration depth of electrons in body tissues is only a fraction of the penetration depth of photons. The results presented in the next two sections clearly reflect these differences.

3.1.1 Photons

Figure 1 shows ratios between effective dose to the MAX-FAX phantoms and effective dose to the ADAM-EVA phantoms for external photon radiation as a function of the incident energy between 10 keV and 10 MeV, for AP-, PA-, and ROT-incidence. The ADAM-EVA data have been taken from ICRP74 (ICRP 1996a), while the MAX-FAX data have been calculated with exposure model c) mentioned in section 2.5. For external exposure to photons the replacement of the stylized exposure models by the voxel-based exposure models leads to a decrease of the effective dose by up to 25% for incident energies above 30 keV. For smaller energies the decrease can be more than 40%.

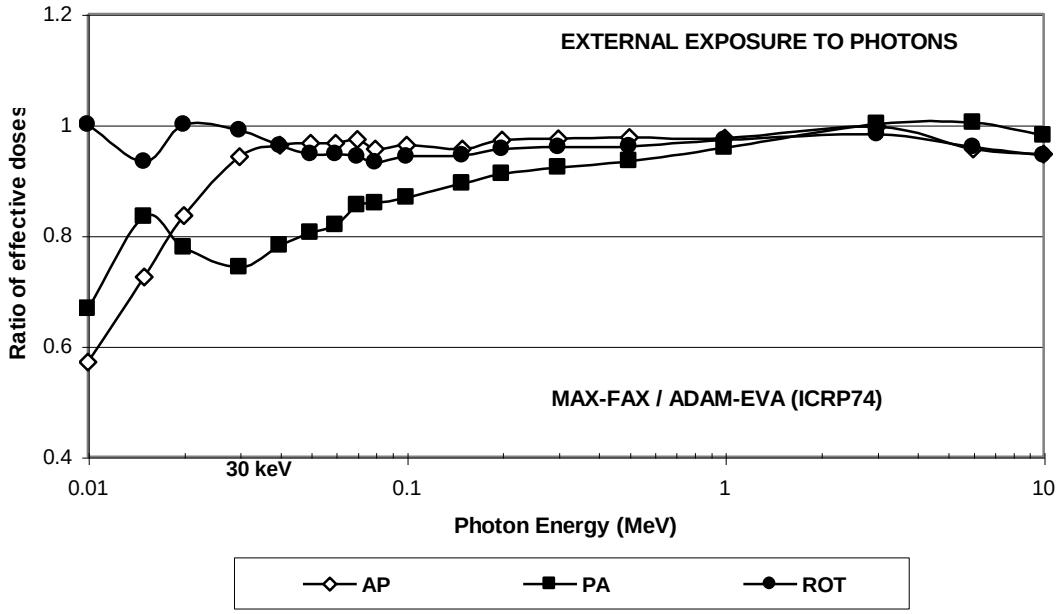

Figure 1. Ratios between effective dose to the MAX-FAX phantoms and effective dose to the ADAM-EVA phantoms for external exposure to photons as function of the incident photon energy for AP-, PA- and ROT incidence.

The effective dose is the sum of weighted equivalent doses to 23 organs and tissues, whose size, form, and location relative to each other determine a complex distribution of organ and tissue equivalent doses as a function of the radiation energy and direction of incidence. In order to understand the decrease of the effective dose shown in figure 1, one has to analyse the change of the equivalent dose to the organs and tissues contributing to the effective dose. At the time when a female adult voxel-based phantom was not available, such an analysis has been reported for the replacement of the ADAM phantom by the MAX phantom (Kramer et al 2004b). Here the analysis will include also the female phantoms EVA and FAX.

The trunks of the ADAM-EVA phantoms are elliptical cylinders with integrated arms and constant thicknesses (values in brackets are for EVA and FAX, respectively) of 20cm (18.8cm) sagittal, and 40cm (37.6cm) lateral, while the MAX-FAX phantoms' body thicknesses vary between 20-24cm (19.5-22cm) sagittal, 50-52cm (43-45cm) lateral in the regions of the upper arms, and 30-33cm (29-31cm) in the abdominal regions, where the lower arms and hands are separated from the trunk. Comparison of cross-sectional images reveal that often the skeletons and internal organs of the MAX and FAX phantoms are surrounded by thicker layers of adipose and muscle compared to the ADAM-EVA phantoms, i.e. many organs in a real human body are

at greater depth than in a stylized phantom. As an example figure 2 shows that especially for AP- and PA-incidence of the radiation the liver and the stomach of the MAX phantom are more shielded by overlying tissues than the liver and the stomach of the ADAM phantom. These anatomical differences combined with a greater density of the muscle regions in the MAX-FAX

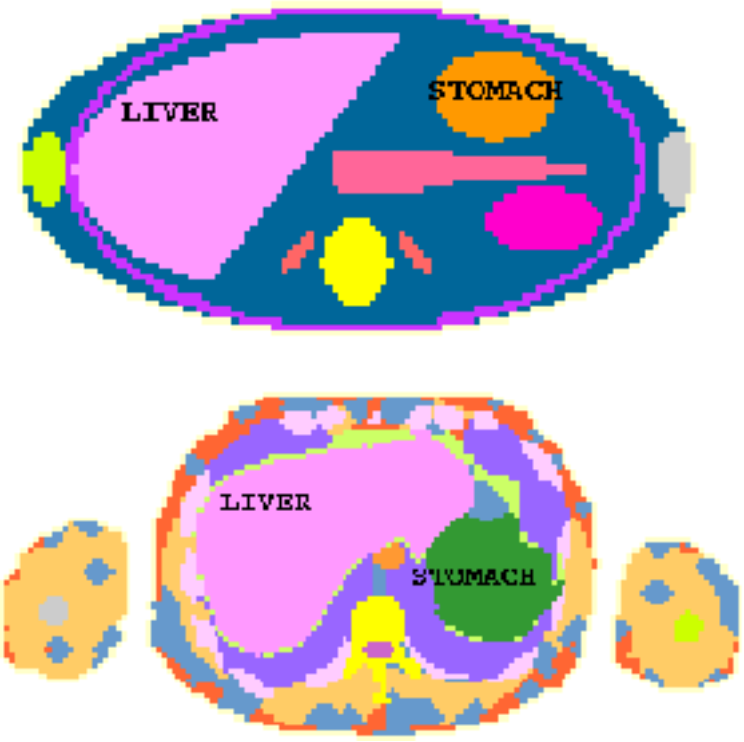

Figure 2. Cross-sectional images of the ADAM (above) and the MAX (below) phantom

phantoms compared to the soft-tissue regions in the ADM-EVA phantoms generally cause more shielding for internal radiosensitive organs. Compared to the stylized skeletons of the ADAM-EVA phantoms, MAX and FAX have naturally structured skeletons with differently shaped pelvises and ribcages with sterni, which provide additional shielding for internal organs.

Considering all 23 organs and tissues mentioned in table 1 for the four phantoms for all energies and directions of incidence would be beyond the scope of this presentation. Therefore table 2 shows ratios between organ equivalent doses for the MAX-FAX and the ADAM-EVA phantoms for AP incidence for energies from 10 to 100 keV as an example. Only those organs and tissues have been included in table 2 whose weighted equivalent doses represent at least 2% of the effective dose of either exposure model. Additionally the last line of table 2 shows the mean free path-length for photons in soft-tissue, which have been calculated based on the mass attenuation coefficients from Hubbell and Seltzer (1996), and which can be considered as an indicator of the penetration depth.

For incident photon energy of 10 keV the testes, the female breast, the skin, and for the stylized phantoms also the thyroid contribute to the effective dose, only the breast equivalent dose of which shows an increase, while the other three organ equivalent doses decrease when the ADAM-EVA phantoms are replaced by the MAX-FAX phantoms. As the weighted testes equivalent dose represents more than 80% of the effective dose, the corresponding ratio in figure 1 shows a decrease of more than 40% at 10 keV. With increasing energy more organs and tissues contribute to the effective dose, and differences between equivalent doses for the stylized and the voxel-based exposure models become smaller. The following description about

anatomical differences between some of the organs and tissues of the two types of phantoms may be helpful to understand the ratios shown in table 2. For energies greater than 300 keV the ratios vary +/-10% around unity.

Table 2. Ratio between MAX-FAX and ADAM-EVA organ equivalent doses for external exposure to photons for AP-incidence and six different incident energies.

ORG / TISS	10 keV	15 keV	20 keV	30 keV	100 keV	300 keV
Testes	0.17	0.56	0.76	0.91	0.96	0.95
Ovaries				1.34	1.04	1.03
RBM		0.75	0.86	1.09	0.99	1.01
Colon			3.53	1.48	1.02	0.95
Lungs			2.20	1.10	0.97	1.02
Stomach		0.38	0.38	0.61	0.85	0.89
Bladder			0.34	0.69	0.92	0.91
Breast	1.59	1.05	1.00	1.05	1.03	1.02
Liver			0.83	0.81	0.93	0.91
Oesophagus				3.10	1.22	1.17
Thyroid		0.33	0.50	0.70	0.83	0.97
Skin	0.97	0.99	0.98	1.03	1.00	1.01
Bone surface			1.04	1.08	1.03	1.00
Remainder		0.17	0.91	0.98	0.96	0.98
MFP [cm]	0.13	0.41	0.84	1.83	4.09	5.90

RBM = red bone marrow, MFP = mean free path-length in soft-tissue

Testes

The thighs of the ADAM phantom are touching, while those of the MAX phantom are partly separated. Consequently the ADAM testes receive more backscattered radiation for AP-incidence than the MAX testes, and on the other hand less unattenuated radiation for PA-incidence because of the shielding by the thighs. All MIRD5-based male phantoms have a so-called "genitalia region" surrounding the testes, which gives rise to additional scattered radiation to the testes especially for AP- and ROT-incidence. Therefore the equivalent dose to the testes decreases for AP- and ROT-incidence when MAX replaces ADAM. The relative increase of the MAX testes equivalent dose for PA-incidence and for low energies is not relevant for the effective dose because the absolute value of the testes equivalent dose is quite small.

Ovaries

The ovaries of the EVA phantom are located at a depth of 9.4cm, whereas in the FAX phantom the ovaries are positioned at a depth of 6.8cm. Therefore the FAX ovaries equivalent dose exceeds the EVA ovaries equivalent dose up to ca. 70 keV for AP-incidence. For PA-

incidence the FAX ovaries receive smaller equivalent doses because they are located deeper inside the body, and also because of additional shielding by the naturally formed pelvis.

Red bone marrow (RBM)

Although both concepts are based on the energy deposition in a homogeneous skeletal mixture, the dosimetric methods for the calculation of equivalent dose to the RBM are quite different for the ADAM-EVA and the MAX-FAX phantoms. These differences refer to the elemental composition of the skeletal tissues and their distribution throughout the skeleton, the photoelectron correction factors, the RBM mass fractions and the cellularity factors. In addition one can observe significant anatomical differences between the stylized and the voxel-based skeletons. A detailed analysis of the impact of these differences on the RBM equivalent dose has been given earlier (Kramer et al 2004b). For the energies and directions of incidence considered here one finds that for AP- incidence the RBM equivalent dose initially decreases for the MAX-FAX phantoms compared to the ADAM-EVA phantoms, while above 30 keV the reverse can be observed. For PA- and ROT- incidence the ADAM-EVA RBM equivalent dose is always greater than the MAX-FAX RBM equivalent dose.

Colon

The ADAM-EVA colons are basically parallelepipeds located at the center of the trunk of the two phantoms, whereas in the MAX-FAX phantoms the colons are located partly in the frontal part, but especially in the rear part of the abdomen. Consequently the voxel-based colons receive a significant equivalent dose already for low energies, i.e. weak penetrating photons below 40 keV, thereby increasing the colon equivalent dose of the MAX-FAX phantoms compared to the ADAM-EVA phantoms. For energies above 100 keV up to ca. 1 MeV the ADAM-EVA colons show higher values than the MAX-FAX colons by ca. 10% because of the the smaller abdominal thicknesses of the ADAM-EVA phantoms, and additionally another 10% because of shielding effects by the pelvis of the MAX-FAX phantoms for PA-incidence.

Lungs

The natural ribcage with its sternum provides for more shielding for the lungs than the equidistant tori of the stylized ribcage. On the other hand, due to the 20% increase of lung mass in ICRP89 (ICRP 2003), the MAX-FAX lungs extend much closer to the phantom's surface, thereby receiving some equivalent dose also for low energies, which explains why the lungs ratios in table 2 are greater than unity. Compared to the MAX-FAX phantoms a significant part of the lungs of the ADAM-EVA phantoms are located in the rear part of the trunk, which leads to higher lung equivalent doses for PA-incidence for the stylized phantoms

Stomach

The stomachs of the ADAM-EVA phantoms are located very close to the frontal surface, and show no extension into the rear part of the body, compared to the MAX-FAX phantoms. Therefore the stomach equivalent dose becomes smaller for AP-incidence. For PA-incidence one finds the reverse situation, but only for low energies up to ca. 35 keV, because the MAX-FAX stomachs extend also somewhat to the frontal part of the body.

Bladder

In the stylized ADAM-EVA phantoms the position of the bladder is about 1 cm below the frontal surface, whereas in the MAX-FAX phantoms the beginning of the bladder wall is located at about 5 cm depth, which leads to a decrease of the bladder equivalent dose for the voxel-based phantoms for AP-incidence.

Breasts

The breasts of both female phantoms have almost the same sagittal thickness, however the EVA breasts have 6.4% more mass, and the FAX breasts are more laterally extended. The breast equivalent doses for AP-incidence are slightly greater for the FAX phantom, except for 10 keV incident photon energy, when the breasts of the FAX phantom receive a significant greater equivalent dose to the breasts because of these anatomical differences and because of the thinner skin thickness.

Thyroid

The thyroid has a very superficial position in the stylized ADAM-EVA phantoms. This leads to significantly smaller thyroid equivalent doses for the MAX-FAX phantoms compared to the ADAM-EVA phantoms for AP-incidence.

Skin

In the stylized ADAM-EVA phantoms the thickness of the skin is 2mm for both models, whereas the voxel-based FAX phantom has a skin thickness of 1.2mm, and the MAX phantom of 1.5mm.

Smaller equivalent doses for the MAX-FAX compared to the ADAM-EVA phantoms can also be found for the liver and many other internal organs for all directions of incidence because of increased shielding by thicker adipose and muscle layers in the voxel-based phantoms, and by the pelvis and the spine of the real human skeleton especially for PA-incidence. For AP-incidence the remainder equivalent dose of the ADAM-EVA phantoms is relatively great, because the very superficially positioned thymus receives a high equivalent dose due to the lack of a sternum in the ribcages of the stylized phantoms. In a real human body many internal organs are positioned at greater depth and/or are more shielded by skeletal structures than in stylized anatomies, at least than those of the MIRD5 type.

3.1.2 Electrons

Figure 3 shows ratios between effective dose to the MAX-FAX phantoms and effective dose to the ADAM-EVA phantoms for external electron radiation as a function of the incident energy between 100 keV and 10 MeV, for AP-, PA- and ROT-incidence. The data for the ADAM-EVA phantoms have been calculated according to exposure model a), while the data for the MAX-FAX phantoms have been calculated according to exposure model c), both mentioned in section 2.5

The skin equivalent dose has been calculated without the 0.007cm surface layer, which is considered to be insensible to ionising radiation. An algorithm introduced into the Monte Carlo code excludes the energy depositions registered in the 0.007cm surface layer. The ratios shown in figure 3 indicate that for external exposure to electrons the effective dose can change between

+26% and –50% when voxel-based exposure models replace stylized exposure models at least for the energies and directions of incidence considered here.

Similar to the approach for external exposure to photons in the previous section, the analysis of the curves presented in figure 3 makes use of ratios between organ equivalent doses for the MAX-FAX and the ADAM-EVA exposure models, which are shown in table 3 for AP-incidence, and again only those organs and tissues have been included, whose weighted equivalent doses contribute by more than 2% to the effective dose.

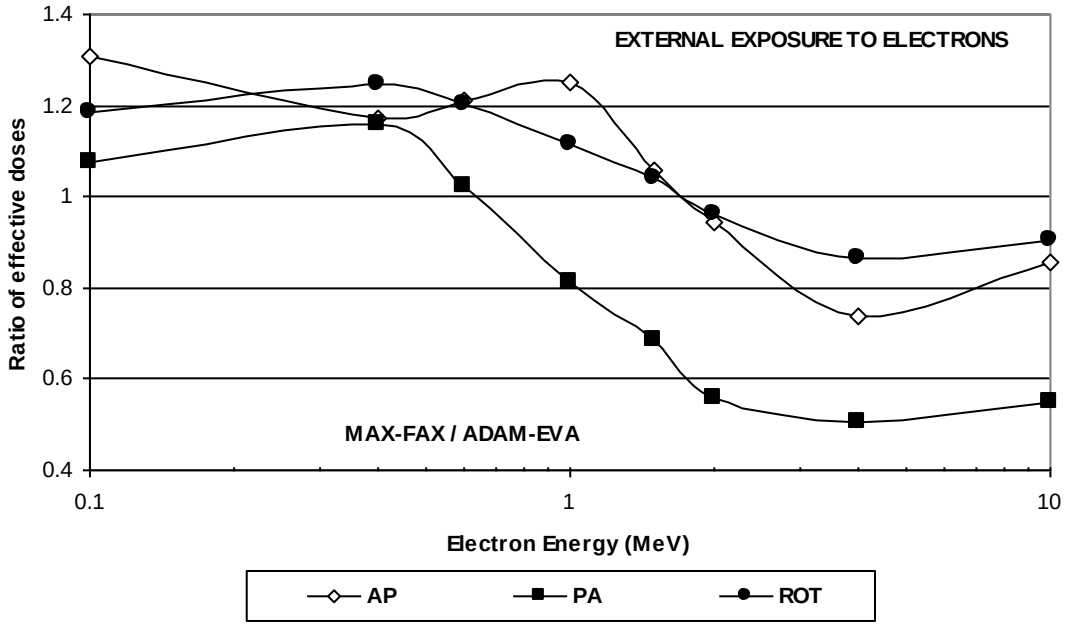

Figure 3. Ratios between effective dose to the MAX-FAX phantoms and effective dose to the ADAM-EVA phantoms for external exposure to electrons as function of the incident photon energy for AP-, PA- and ROT-incidence.

While the anatomical differences between the two types of phantoms described in the previous section apply to electrons as well, the main distinction to be taken into account here is the much smaller range of electrons compared to photons for a given energy. Therefore the last line of table 3 shows additionally CSDA ranges for electrons in soft tissue as a function of the incident energy (Hubbell and Seltzer 1996). In soft-tissue 10 keV photons have a mean free path-length of 1.3mm, while the incident energy of electrons has to be 400 keV to cross through the same thickness, or for an incident energy of 100 keV the CSDA range of an electron is about 1/400 of the mean free path-length of a photon with the same energy.

For electron energies up to 1 MeV the only relevant contributors to the effective dose are the skin, the female breasts and the testes, the skin equivalent dose of which represents more than 90% of the effective dose. The equivalent doses to these organs are mostly greater in the MAX-FAX phantoms than in the ADAM-EVA phantoms, and consequently the ratio for AP-incidence in figure 3 shows values well above unity for this range of energies with a maximum of 1.3 at 100 keV. The reasons are the ‘genitalia region’ surrounding the ADAM testes, which has to be traversed by the electrons before they reach the testes, the greater lateral extension of the FAX breasts, and the thinner skin of the FAX phantom, which indirectly increases additionally the equivalent dose to the breasts. Above 1.0 MeV the effective dose ratio for AP-incidence starts to decrease, because the MAX-FAX skin and testes equivalent doses become smaller than the ADAM-EVA skin and testes equivalent doses, and additionally reduction of the effective dose ratio is caused by the RBM and the thyroid. The ratio arrives at a minimum of

0.74 at 4 MeV and then starts to increase again. The organs and tissues contributing to the effective dose shown in table 3 are basically the same reported by a similar table for external exposure to electrons published in ICRP74 (ICRP 1996a).

Table 3. Ratio between MAX-FAX and ADAM-EVA organ equivalent doses for external exposure to electrons as a function of the particle energy and for AP-incidence.

ORGAN / TISSUE	100 keV	400 keV	600 keV	1.0 MeV	1.5 MeV	2.0 MeV	4.0 MeV	10.0 MeV
Testes			3.70	2.93	0.80	0.71	0.71	0.89
Ovaries								
RBM					0.25	0.24	0.44	0.95
Colon								5.29
Lungs							1.04	1.64
Stomach								0.31
Bladder								0.15
Breast	1.48	1.20	3.08	2.23	1.50	1.33	1.12	1.00
Liver								0.57
Oesophagus								
Thyroid						0.24	0.22	0.76
Skin	1.17	1.22	1.00	0.83	0.94	0.94	0.94	0.82
Bone surface								
Remainder								
CSDA Range [cm]	0.01	0.13	0.23	0.44	0.71	0.98	2.05	5.01

RBM = red bone marrow, CSDA = Continuous Slowing Down Approximation in soft-tissue

Table 4. Ratio between MAX-FAX and ADAM-EVA organ equivalent doses for external exposure to electrons as a function of the particle energy and for PA-incidence.

ORGAN / TISSUE	100 keV	400 keV	600 keV	1.0 MeV	1.5 MeV	2.0 MeV	4.0 MeV	10.0 MeV
Testes					33.3	30.0	47.2	2.0
Ovaries							0.73	1.0
RBM				0.31	0.1	0.1	0.2	0.5
Colon						3.1	7.9	14.4
Lungs							0.38	0.39
Stomach								2.13
Bladder								
Breast								
Liver								0.76
Oesophagus								
Thyroid								
Skin	1.08	1.22	0.99	0.79	0.84	0.84	0.91	0.96
Bone surface							0.43	0.61
Remainder								
CSDA Range [cm]	0.01	0.13	0.23	0.44	0.71	0.98	2.05	5.01

RBM = red bone marrow, CSDA = Continuous Slowing Down Approximation in soft-tissue

Table 4 shows ratios between organ equivalent doses for the MAX-FAX and the ADAM-EVA exposure models for PA-incidence as a function of the incident electron energy. Below 1 MeV the effective dose is almost identical with the skin equivalent dose, because now the breasts are shielded by the trunk, and the testes at least partly by the thighs.

The curve for PA-incidence in figure 3 has almost the same shape as the curve for AP-incidence, however with a smaller maximum of about 1.16 at 400 keV, but on the other hand with a greater minimum of about 0.5 at 4 MeV incident energy. Deviation from AP- and PA-incidence leads to a reduction of the maximum as well as of the minimum of the effective dose ratio. For a full rotation in a broad beam of electrons (ROT-incidence) the effective dose varies between +25% and –16% when the stylized ADAM-EVA phantoms are replaced by the voxel-based MAX-FAX phantoms.

3.2 Internal exposures

Effective doses per cumulated activity have been calculated for gamma and beta emitters homogeneously distributed in the liver, the lungs, the skeleton, the thyroid, the kidneys and the spleen of the MAX-FAX and the ADAM-EVA phantoms for energies between 10 keV and 4 MeV. The remainder equivalent dose has been calculated according to ICRP68 (ICRP 1995a), which recommends the mass-weighted average of the contributing organ and tissue equivalent doses, also taking into account footnote 3 of Table 2 from ICRP60 (ICRP 1991), i.e. that if the equivalent dose of one of the remainder organs or tissues is greater than the maximum equivalent dose of the main organs or tissues, then half of the remainder weighting factor should be applied to the equivalent dose of that remainder organ or tissue, while the other half should be used for the arithmetic average of the equivalent dose of the remaining organs or tissues. For very small equivalent doses, if the coefficient of variance (CV) of the equivalent dose to an organ or tissue mentioned in table 1 was greater than 30%, then its equivalent dose was disregarded in the calculations.

Exposure to photons or electrons from incorporated radionuclides usually causes the greatest equivalent dose in the source organ, which for very low energies absorbs almost all radial energy. For a given energy of the source particles the equivalent doses to other organs and tissues are mainly a function of the distance between the source and the target organs, and of the type of source particle. Because of the differences with respect to the range mentioned above, for a given energy exposure to internally emitted photons is expected to affect more target organs in the vicinity compared to the case when the incorporated radionuclides emit electrons.

3.2.1 Gamma emitters

Figure 4 shows ratios between effective doses for the MAX-FAX and for the ADAM-EVA phantoms for photon emitters homogeneously distributed in the liver, the lungs, the skeleton, and the thyroid as a function of the emitted energy between 10 keV and 4 MeV calculated according to exposure models c) and a).

In contrast to the findings for external exposures in figure 1, for internal exposures to photons the introduction of a real human anatomy generally leads to an increase of the effective dose by up to 60%, 37%, 25% or 15% when the liver, the skeleton, the lungs or the thyroid is the source organ, respectively. The equivalent dose to the source organ itself may increase or decrease especially for very low energies because of differences of mass or density, however, with increasing energy almost all organ and tissue equivalent doses increase, because most distances between organs in a real human body are shorter compared to the inter-organ distances in the stylized phantoms.

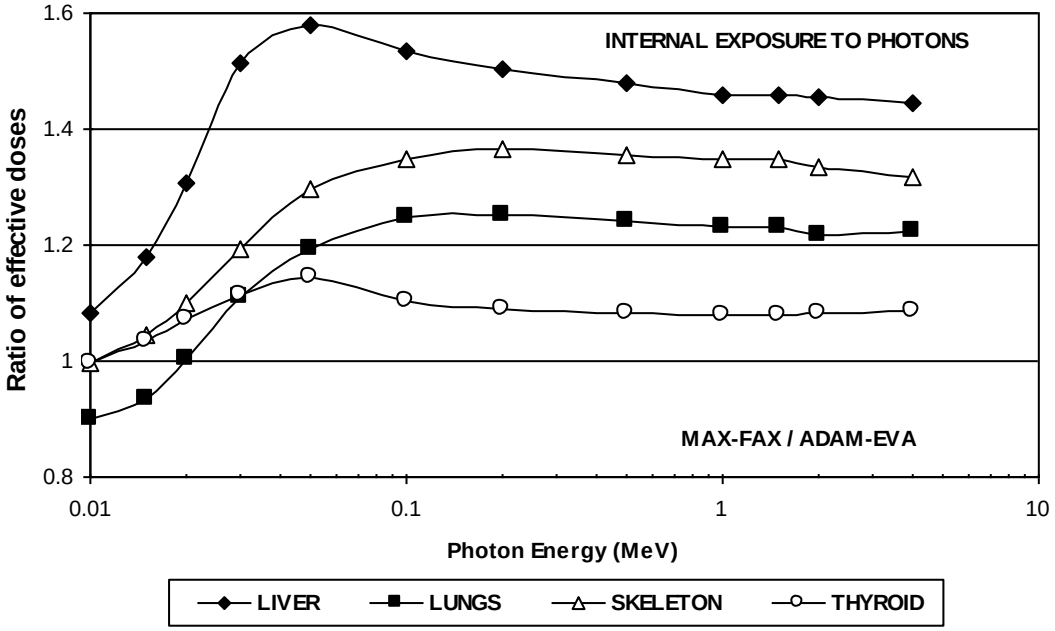

Figure 4. Ratios between effective dose to the MAX-FAX phantoms and effective dose to the ADAM-EVA phantoms for internal exposure to photons as function of the emitted energy for the source organs liver, lungs, skeleton and thyroid

Table 5 shows ratios between organ and tissue equivalent doses for the MAX-FAX and the ADAM-EVA phantoms for the source organ liver as a function of the emitted photon energy for those organs and tissues whose weighted equivalent doses contribute by at least 2% to the effective doses. The equivalent dose to the source organ does not change very much by introducing a real human liver, but significant increases can be observed for all organs and tissues in the vicinity of the liver, except for the ovaries.

Table 5. Ratio between MAX-FAX and ADAM-EVA organ equivalent doses for internal exposure to photons as a function of the emitted energy, when the liver is the source organ.

ORGAN / TISSUE	10 keV	30 keV	50 keV	100 keV	500 keV	1.0 MeV
Testes						
Ovaries				0.80	0.905	0.886
RBM			1.58	1.67	1.8	1.8
Colon		7.08	3.82	2.92	2.64	2.6
Lungs		1.51	1.39	1.44	1.49	1.43
Stomach		7.92	3.87	2.93	2.83	2.82
Bladder						
Breast			2.31	1.88	1.71	1.65
Liver (source)	1.00	1.06	1.14	1.13	1.07	1.07
Oesophagus						
Thyroid						3.25
Skin						
Bone surface						
Remainder						

RBM = red bone marrow

In a real human body the liver as one of the largest organs has close contact with other organs, like the stomach, the colon, the lungs and bones of the ribcage, whereas in stylized phantoms these organs are quite separated from each other. This might be a consequence when trying to position the rigid geometrical forms (circular and elliptical cylinders, spheres, cones, tori, etc.) of these organs in an anatomically correct manner, because it is almost impossible to assemble those geometrical forms close to each other the way these organs appear in a real human body.

3.2.2 Beta emitters

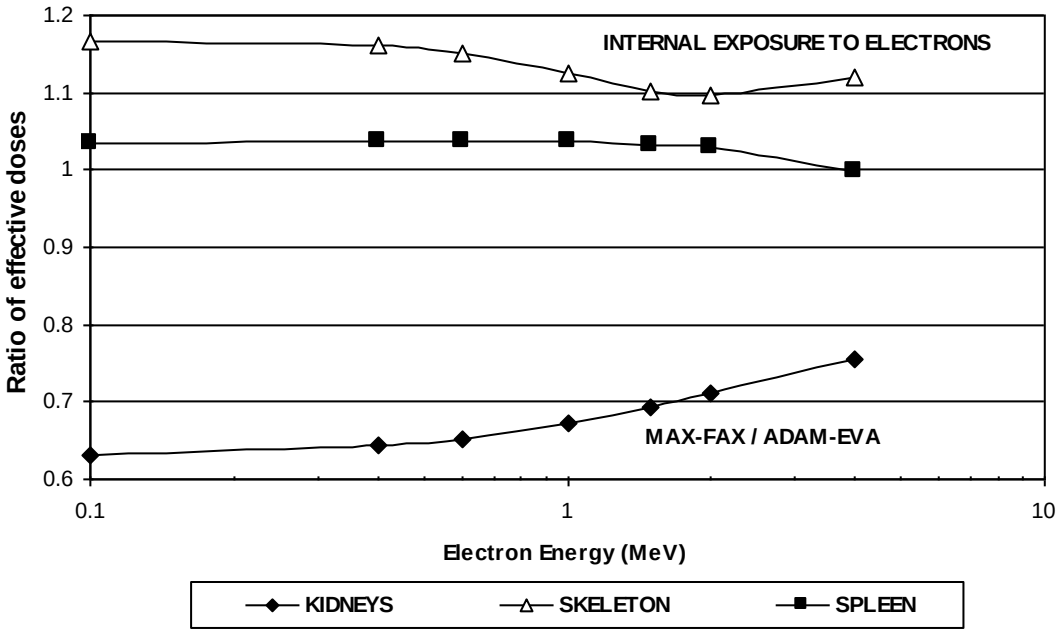

Figure 5. Ratios between effective dose to the MAX-FAX phantoms and effective dose to the ADAM-EVA phantoms for internal exposure to electrons as function of the emitted energy for the source organs kidneys, skeleton and spleen

Figure 5 shows ratios between effective doses for the MAX-FAX and for the ADAM-EVA phantoms for beta emitters homogeneously distributed in the kidneys, the skeleton, and the spleen as a function of the energy between 100 keV and 4 MeV, calculated according to exposure models c) and a).

Introduction of a real human anatomy generally leads to an increase of the effective dose, an observation already made in figure 4 for internal photon emitters. The reasons are the shorter distances between organs in a real human body compared to the inter-organ distances in the MIRD5-type phantoms. Figure 5 shows increases by up to 17% for the skeleton effective dose, and by up to 3.5% for the spleen effective dose. However, the increases of the effective dose in case of internal electron emitters are usually smaller because of the smaller range of the electrons compared to photons for a given energy. The decrease of up to 37% of the effective

dose for the source organ kidneys in figure 5 is due to the presence of voxels of urine in the kidneys of the MAX-FAX phantoms. A part of the energy emitted from the radionuclides in the cortex of the MAX-FAX kidneys is absorbed in the urine voxels, i.e. that this energy does not contribute to the equivalent dose for the kidneys. As the "cortex kidneys" of the voxel phantoms have almost the same mass as the kidneys of the ADAM-EVA phantoms, the effective doses per cumulated activity for the MAX-FAX phantoms become smaller which is reflected in figure 5 by the low ratio for the kidneys.

Table 6 shows ratios between organ equivalent doses for the MAX-FAX and the ADAM-EVA phantoms for the source organ skeleton as a function of the emitted electron energy for those organs and tissues whose weighted equivalent doses contribute by at least 2% to the effective doses. For a given energy the range of beta particles in bone is much smaller than in soft-tissue, and consequently only relatively few electrons leave the skeleton in order to deposit energy in the vicinity. Additionally this vicinity is mostly made of skeletal muscle, which means that only few soft-tissue organs are close enough to skeletal structures to receive a significant equivalent dose as target organs. Therefore by far the greatest part of the emitted energy is absorbed in bone and bone marrow.

Table 6. Ratio between MAX-FAX and ADAM-EVA organ equivalent doses for internal exposure to electrons as a function of the emitted energy, when the skeleton is the source organ.

ORGAN / TISSUE	100 keV	400 keV	600 keV	1.0 MeV	1.5 MeV
Testes					
Ovaries					
RBM	0.93	0.89	0.88	0.93	0.86
Colon					
Lungs	46.03	41.25	37.84	30.44	23.85
Stomach		63.64	32.26	18.28	26.00
Bladder					
Breast					
Liver					
Oesophagus			4.73	3.57	2.85
Thyroid					
Skin					
Bone surface	0.92	0.90	0.90	0.92	0.90
Remainder					

RBM = red bone marrow

The average density of the MAX-FAX skeletons is about 3.5% smaller than the density of the ADAM-EVA skeletons, which causes a decrease of the equivalent dose to the bone surface and to the RBM. On the other hand one can observe an increase of equivalent dose for the lungs, the stomach and the oesophagus because in the MAX-FAX phantoms these organs are located closer to skeletal structures than in the ADAM-EVA phantoms.

3.3 Comparison with other investigations

With respect to the calculational methods used in this investigation, i.e. the application of the EGS4 Monte Carlo code to equivalent dose determination in human phantoms, extensive comparisons have been made with data published by the ICRP and excellent agreements have been found (Kramer et al 2005a,b,c, Lima et al 2005). With respect to comparisons between equivalent doses for voxel-based and stylized exposure models other investigations are reviewed in the following sections. The majority of studies found on this subject deals with exposure to photons.

3.3.1 External exposures

3.3.1.1 Photons

Jones (1995,1997) published two papers which, among other aspects, investigate also effective dose differences between the NORMAN voxel phantom (Dimbylow 1995) and the ADAM phantom for external exposure to photons for the field geometries mentioned above. The radiation transport code, the RBM model and the representation of the skeleton were the same for both phantoms. For incident photon energies above 25 keV, and for AP-, PA-, and ROT-incidence Jones found a maximum decrease of 22% of the effective dose due to the replacement of the stylized anatomy by a voxel-base anatomy.

Chao et al (2001a) compared the VIP-Man (Xu et al 2000) effective dose with the ADAM-EVA effective dose for external exposure to photons. Here not only the two exposure models were different with regard to the radiation transport code, to the tissue compositions, to the RBM model, and to the representation of the skeleton, but the two quantities to be compared were different too. The ADAM-EVA effective dose is a quantity averaged over both genders, while the VIP-Man effective dose belongs to an adult male. For incident photon energies above 30 keV Chao et al found an increase of the VIP-Man effective dose by up to 30% for AP-, and ROT-incidence, and a decrease by up to 125% for PA-incidence when the voxel-based model replaced the stylized models.

Zankl et al (2002) published a comprehensive comparison of organ and tissue CCs for external photon exposures between a whole family of voxel phantoms, and the mathematical ADAM and EVA phantoms. The radiation transport code applied was the same for all phantoms, the tissue compositions were different, and so were the RBM models and the representation of the skeleton. For incident energies above 30 keV Zankl et al found a decrease by up to 20% for the effective dose when voxel-based models replace the ADAM-EVA phantoms.

3.3.1.2 Electrons

Chao et al (2001b) calculated conversion coefficients between organ equivalent dose and incident electron fluence for the voxel-based VIP-Man phantom, but no data were given for the effective dose. However, using the data published by Chao et al it was possible to calculate a VIP-Man effective dose based on the organ equivalent dose conversion coefficients according to quation (2) from section 2.6 if one uses only the male contribution E_M. Correspondingly also the MAX effective dose and the ADAM effective dose have been calculated.

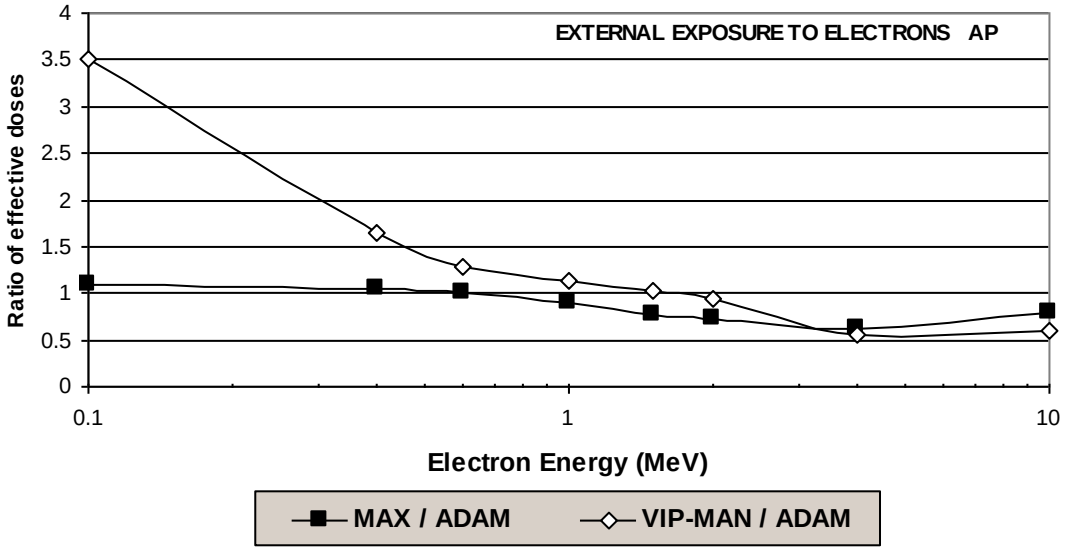

Figure 6. Ratios between male effective doses to the MAX and to the ADAM phantoms, and between male effective doses to the VIP-Man and to the ADAM phantoms.

Figure 6 shows ratios between the male effective doses for the MAX and the ADAM phantoms, and between the male effective doses for the VIP-Man and the ADAM phantom. In view of the differences between the VIP-Man and the MAX phantoms with regard to body height, body weight, organ masses, RBM dosimetry, etc., acceptable agreement within a margin of less than 28% can be observed between the two ratios for incident electron energies above 600 keV. For lower energies the VIP-Man/ADAM ratio is significantly greater than the MAX/ADAM ratio, because both exposure models use different thicknesses for the skin. The skin thickness of the ADAM phantom is 2mm with the exclusion of the superficial layer of 0.007cm, whereas "for the VIP-Man, the skin is defined as the combination of …. two layers, which is about 0.7mm thick in the front surface of the body and more than 0.7 mm on other parts of the body" (Chao 2001b), which leads to greater skin equivalent doses for the VIP-Man phantom for low energies at least for AP-incidence. Table 3 of this study shows that for a male phantom irradiated with electrons of energy below 600 keV the effective dose is practically equal to the skin equivalent dose. Therefore one can expect agreement between the two ratios in figure 6 also for energies below 600 keV if the VIP-Man and the ADAM phantom would use the same representation of the skin.

3.3.2 Internal exposures

3.3.2.1 Gamma emitters

Jones (1998) compared Specific Absorbed Fractions (SAFs) calculated for the NORMAN voxel phantom (Dimbylow 1995) with corresponding data for the MIRD5 phantoms (Cristy and Eckerman 1987). The results showed sometimes significant differences between the SAFs of the two exposure models. Jones' calculations demonstrated that a change of the tissue composition had only little effect on the results, and he concluded that especially different inter-organ distances in the two phantoms were the main cause of the large discrepancies found between the SAF values. Differences in organ and tissues masses could not have been the reason, because

both phantoms had organ and tissue masses which agreed fairly well with the reference masses of ICRP23.

Significant discrepancies between MIRD5 and voxel-based SAFs have also been reported by Petoussi-Henss and Zankl (1998), by Smith et al (2000), by Yoriyaz et al (2000), by Smith et al (2001), by Stabin and Yoriyaz (2002) and by Zankl et al (2003), confirming that the voxel-based SAFs are often significantly greater than the MIRD5 SAFs, and that such large discrepancies typically do not appear for the source organ itself. These authors conclude that the generally smaller distances between source and target organs in voxel-based phantoms are the reason for the increase of equivalent dose.

3.3.2.2 Beta emitters

Specific absorbed fractions from internal electron emitters have been calculated by Chao et al (2001c) for the voxel-based VIP-Man phantom, but unfortunately the results do not include the effective dose, and no comparison with MIRD5-type phantoms was made. Kinase et al (2004) calculated S values for Beta-ray emitters in the bladder for the MIRD5 and for two voxel-based phantoms, however the comparison took only the source organ into account, and neither equivalent dose to other target organs nor the effective dose have been considered.

4. Conclusions

The purpose of this study was to investigate the dosimetric consequences if voxel-based exposure models will replace the traditional stylized exposure models. Although different Monte Carlo codes and tissue compositions can influence the results of equivalent dose calculations in human phantoms this investigation has shown, that the introduction of real human anatomies is mainly responsible for the changes observed for equivalent doses to organs and tissues of the human body.
For external exposures two principal reasons have been identified:

- In voxel-based phantoms many internal soft-tissue organs are located at deeper positions below the surface compared to their location in the stylized phantoms, which is equivalent to the conclusion that in voxel-based anatomies these organs are more shielded by layers of adipose and muscle.
- The real human skeleton provides more shielding for internal organs than the skeleton of the stylized phantoms

For internal exposures the main reasons are the smaller distances between internal organs in real human bodies compared to the inter-organ distances in stylized phantoms.

In radiological protection the effective dose is the most important quantity. Therefore this study was focussed on organ and tissue equivalent dose calculations with voxel-based and stylized exposure models in order to see how the effective dose would change. In particular the voxel-based MAX and FAX phantoms and the stylized ADAM and EVA phantoms have been used to calculate effective doses for external and internal exposures to photons and electrons. The ratios between the effective doses for the voxel-based and the stylized exposure models presented show that for the irradiation conditions considered in this study the effective dose to voxel models

- may decrease by up to 40% for external exposures to photons,

- may vary between +26% and – 50% for external exposures to electrons,
- may increase by up to 60% for internal exposures to photons, and
- may vary between –37% and +17% for internal exposure to electrons.

As sum over 23 weighted organ and tissue equivalent doses the effective dose is usually the result of a complex distribution of equivalent dose throughout the body, and therefore its interpretation is sometimes not so obvious, and the interpretation of the ratio of two effective doses from two different exposure models does not make things easier. In order to facilitate the interpretation of the effective dose ratios presented in figures 1, and 3 to 5, tables 2 to 6 were compiled, which show ratios between organ and tissue equivalent doses of the voxel-based and the stylized exposure models observing the condition that the weighted organ or tissue equivalent dose must contribute by at least 2% to the effective dose. Although the CVs for single organs and tissues can sometimes show double digit number, these tables are useful tools for the analysis of the effective dose ratios, because they indicate the direction of change for the organ or tissue equivalent dose under consideration, and at the same time they explain which organs or tissues contribute significantly to the effective dose for a given energy, direction of incidence, source organ, etc.

In radiological protection from external exposures rotational or semi-rotational incidence are more likely than exact AP- or PA-incidence. Additionally photon energies are found mostly in the range above 30 keV. Therefore one can conclude that for most practical situations for external exposures to photons the reduction of the effective dose due to the introduction of voxel-based models rarely exceeds 10%. Similar considerations for external exposures to electrons suggest that for most practical situations the effective dose would vary between +/- 20% due to the introduction of voxel-based models.

For internal exposures it is not possible to make such generalisations. The possible change of the effective dose depends very much on the source organ under consideration, and the data shown in figures 4 and 5 demonstrate that different source organs can cause significantly different changes of the effective dose.

Along the chain of events from the radiation source to potential health effects, anatomical differences between exposed persons are only one of many influencing factors. Others are the use of area or personal radiation detectors, which can involve uncertainties of 50% or more depending on the knowledge about the exposure conditions, or the derivation of the tissue weighting factors included in the definition of the effective dose, which are based on data with sometimes large statistical variations especially for low doses. The data presented here have shown that for most practical cases of external exposure to photons and electrons the uncertainties for the effective dose due to anatomical variations are about +/- 20%, which perhaps seems negligible compared to other uncertainties. Was it then worth the effort that was made to determine this result ? The answer is yes, because at least otherwise one would not know that the influence of anatomical differences can sometimes be neglected !

Occasionally the question is raised if one could avoid the complicated and time-consuming segmentation of images by making the MIRD5-based phantoms anatomically more realistic. The problem with the MIRD5 concept is that the mathematical equations would become very complicated, if definable at all, when one tries to model the shape of internal organs in a more realistic manner. Voxel phantoms are not only true to nature representations of the human body, but they also allow to determine the maximum absorbed dose, absorbed dose distributions, isodoses, etc. in special regions of the body, or within organs, which is important

for the simulation of radiological accidents (Kramer et al 2005d). Meanwhile voxel phantoms are considered as a progress in the development of human anthropomorphic phantoms, a view which is supported last but not least by the ICRP, which is currently preparing voxel-based reference phantoms

5. Acknowledgement

The authors would like to thank CNPq and FACEPE for financial support.

6. References

Briesmeister J F et al 2000 MCNP: A General Monte Carlo N-Particle Transport Code Version 4C. Edited by J F Briesmeister, Report No. LA-13709-M, Los Alamos Scientific Laboratory, Los Alamos, NM, USA

Chao T C, Bozkurt A and Xu X G 2001a Conversion Coefficients Based on the VIP-Man Anatomical Model and EGS4-VLSI Code for External Monoenergetic Photons from 10 keV to 10 MeV Health Physics 81(2):163-183

Chao T C, Bozkurt A and Xu X G 2001b Organ Dose Conversion Coefficients for 0.1 –10 MeV Electrons Calculated for the VIP-Man Tomographic Model, Health Physics 81(2):203-214

Chao T C and Xu X G 2001c Specific Absorbed Fractions from the Image-based VIP-Man body model and EGS4-VLSI Monte Carlo code: Internal Electron Emitters, Phys.Med.Biol. 46 901-927

Cristy M 1980 Mathematical phantoms representing children at various ages for use in estimates of internal dose Report ORNL/NUREG/TM-367, Oak Ridge National Laboratory, Oak Ridge, TN, USA

Cristy M and Eckerman K F 1987 Specific Absorbed Fractions of Energy at Various Ages from Internal Photon Sources, ORNL/TM-8381 Vol. 1-7,Oak Ridge National Laboratory, Oak Ridge, TN, USA

Dimbylow, P J 1995 The development of realistic voxel phantoms for electromagnetic field dosimetry In: Proceedings of an International Workshop on Voxel Phantom Development held at the National Radiological Protection Board, Chilton, UK, 6-7 July

Fisher H L and Snyder W S 1967 Distribution of dose in the body from a source of gamma rays distributed uniformly in an organ, Report No ORNL-4168, Oak Ridge National Laboratory, Oak Ridge, Tenn, USA

Fisher H L and Snyder W S 1968 Distribution of dose in the body from a source of gamma rays distributed uniformly in an organ Proceedings of the First International Congress on Radiation Protection, Pergamon Press, Oxford, pp 1473-1486

Hubbell J H and Seltzer S M 1996 Tables of X-Ray Mass Attenuation Coefficients and Mass Energy-Absorption Coefficients, Ionizing Radiation Division, Physics Laboratory, National Institute of Standards and Technology, Gaithersburg, MD, USA http://physics.nist.gov/PhysRefData/XrayMassCoef/cover.html

ICRP 1975 Report of the task group on reference man (ICRP Publication 23) (Oxford: Pergamon)

ICRP 1991 1990 Recommendations of the International Commission on Radiological Protection (ICRP Publication 60) (Oxford: Pergamon)

ICRP 1995a Dose Coefficients for Intakes of Radionuclides by Workers (ICRP Publication 68) (Oxford: Pergamon)

ICRP 1995b Basic Anatomical and Physiological Data for Use in Radiological Protection: The Skeleton (ICRP Publication 70) (Oxford: Pergamon).

ICRP 1996a Conversion Coefficients for use in Radiological Protection against External Radiation (ICRP Publication 74) (Oxford: Pergamon)

ICRP 1996b Age-dependent Doses to Members of the Public from Intake of Radionuclides: Part 5 Compilation of Ingestion and Inhalation Coefficients (ICRP Publication 72) (Oxford: Pergamon)

ICRP 2003 Basic Anatomical and Physiological Data for Use in Radiological Protection: Reference Values (ICRP Publication 89) (Oxford: Pergamon)

ICRU 1989 Tissue Substitutes in Radiation Dosimetry and Measurement ICRU Report No. 44. International Commission On Radiation Units And Measurements, Bethesda, MD, USA

Jones D G 1995 Use of voxel phantoms in organ dose calculations, In: Proceedings of an International Workshop on Voxel Phantom Development held at the National Radiological Protection Board, Chilton, UK, 6-7 July

Jones D G 1997 A Realistic Anthropomorphic Phantom For Calculating Organ Doses Arising From External Photon Irradiation, Rad. Prot. Dos. 72, No.1, pp. 21-29

Jones D G 1998 A realistic Anthropomorphic Phantom for Calculating Specific Absorbed Fractions of Energy from Internal Gamma Emitters, Rad. Prot. Dos. 79, Nos.1-4, pp. 411-414

Kinase S, Zankl M, Funabiki J, Noguchi H and Saito K 2004 Evaluation of S Values for Beta-ray Emitters within the Urinary Bladder Paper presented at the 11th Congress of the International Radiation Protection Association, IRPA 11, Madrid, 23-28 May

Kramer R and Drexler G 1982 On the Calculation of the Effective Dose Equivalent Rad. Prot. Dos., 3 13-24

Kramer R, Zankl M, Williams G and Drexler G 1982 The calculation of dose from external photon exposures using reference human phantoms and Monte Carlo methods. Part I: The male (ADAM) and female (EVA) adult mathematical phantoms GSF-Report S-885, Institut für Strahlenschutz, GSF-Forschungszentrum für Umwelt und Gesundheit, Neuherberg-Muenchen

Kramer R, Vieira J W, Khoury H J, Lima F R A and Fuelle D 2003 All About MAX: a Male Adult voXel Phantom for Monte Carlo Calculations in Radiation Protection Dosimetry, Phys. Med. Biol., 48, No. 10, 1239-1262

Kramer R, Vieira J W, Khoury H J, Lima F R A, Loureiro E C M, Lima V J M and Hoff G 2004a All about FAX: a Female Adult voXel Phantom for Monte Carlo Calculation in Radiation Protection Dosimetry, Phys. Med. Biol. 49, 5203-5216

Kramer R, Vieira J W, Khoury H J and Lima F R A 2004b MAX meets ADAM: a Dosimetric Comparison Between a Voxel-Based and a Mathematical Model for External Exposures to Photons, Phys. Med. Biol., 49, 887-910

Kramer R, Khoury H J, Vieira J W, Yoriyaz H and Lima F R A 2005a Effective Dose Ratios for Tomographic and Stylized Models from External Exposure to Photons Paper presented at the Monte Carlo Topical Meeting, Chattanooga, TN, USA, April 17-21

Kramer R, Khoury H J, Vieira J W, Yoriyaz H, Loureiro E C M and Lima F R A 2005b Effective Dose Ratios for Tomographic and Stylized Models from External Exposure to Electrons Paper presented at the Monte Carlo Topical Meeting, Chattanooga, TN, USA, April 17-21

Kramer R, Khoury H J, Vieira J W, Lima F R A and Loureiro E C M 2005c Effective Dose Ratios for Tomographic and Stylized Models from Internal Exposure to Electrons Paper presented at the Monte Carlo Topical Meeting, Chattanooga, TN, USA, April 17-21

Kramer R, A M Santos, C A O Brayner, H J Khoury, J W Vieira and F R A Lima 2005d Application of the MAX/EGS4 exposure model to the dosimetry of the Yanango radiation accident, Phys. Med. Biol. 50, 3681-3695

Lima F R A, Kramer R, Khoury H J, Santos A M, Viera J W 2005 Effective Dose Ratios for Tomographic and Stylized Models from Internal Exposure to Photons Paper presented at the Monte Carlo Topical Meeting, Chattanooga, TN, USA, April 17-21

Nelson W R, Hirayama H and Rogers D W O 1985 The EGS4 Code System SLAC-265, Stanford Linear Accelerator Center, Stanford University, Stanford, CA,USA

Petoussi-Henss N and Zankl M 1998 Voxel Anthropomorphic Models as a Tool for Internal Dosimetry Rad. Prot. Dos. Vol.79, Nos 1-4, pp. 415-418

Smith T, Petoussi-Henss N and Zankl M 2000 Comparison of internal radiation doses estimated by MIRD and voxel techniques for a "family" of phantoms Eur. J Nucl Med 27:1387-1398

Smith T, Phipps A W, Petoussi-Henss N and Zankl M, 2001 Impact on Internal Doses of Photon SAFs Derived with the GSF Adult Male Voxel Phantom Health Physics, Vol. 80 No.5 477- 485

Snyder W S, Ford M R, Warner G G and Watson S B 1974 Revision of MIRD pamphlet no. 5 entitled 'Estimates of absorbed fractions for monoenergetic photon sources uniformly distributed in various organs of a heterogeneous phantom' Report No ORNL-4979, Oak Ridge National Laboratory, Oak Ridge, TN,USA

Snyder W S, Ford M R, Warner G G and Watson S B 1975 Absorbed Dose per Unit Cumulated Activity for Selected Radionuclides and Organs MIRD pamphlet No.11, Society of Nuclear Medicine, New York,USA

Snyder W S, Ford M R and Warner G G 1978 Estimates of absorbed fractions for monoenergetic photon sources uniformly distributed in various organs of a heterogeneous phantom MIRD pamphlet no.5, (revised) Society of Nuclear Medicine, New York,USA

Stabin M, Watson E, Cristy M, Ryman J, Eckerman K, Davis J, Marshall D and Gehlen K 1995 Mathematical models and specific absorbed fractions of photon energy in the nonpregnant adult female and at the end of each trimester of pregnancy Report No. ORNL/TM-12907, Oak Ridge National Laboratory, Oak Ridge, TN, USA

Stabin M G and Yoriyaz H 2002 Photon Specific Absorbed Fractions Calculated in the Trunk of an Adult Male Voxel-Based Phantom Health Physics 82(1): 21-44

Xu X G, Chao T C and Bozkurt A 2000 VIP-MAN: An Image-based Whole-body Adult Male Model Constructed From Colour Photographs Of The Visible Human Project For Multi-particle Monte Carlo Calculations Health Physics 78(5):476-486

Yoriyaz H, Santos A, Stabin M G and Cabezas R 2000 Absorbed fractions in a voxel-based phantom calculated with the MCNP-4B code Med Phys 27(7)1555-1562

Zankl M and Wittmann A 2001 The adult male voxel model GOLEM segmented from whole-body CT patient data", Radiat Environ Biophys, 40: 153-162

Zankl M, Fill U, Petoussi-Henss N and Regulla D 2002 Organ dose conversion coefficients for external photon irradiation of male and female voxel models, Phys Med Biol 47, No.14, 2367-2386

Zankl M, Petoussi-Henss N, Fill U, Regulla D 2003 The Application of Voxel Phantoms to the Internal Dosimetry of Radionuclides Rad. Prot. Dos. Vol. 105, No 1-4, 539-548

Zubal I G, Harrell C R, Smith E O, Rattner Z, Gindi G, Hoffer P B 1994 Computerized three-dimensional segmented human anatomy, Med.Phys. 21 No.2, 299-302